Chinese Journal of Natural Medicines

Five new terpenoids from *Viburnum odoratissimum* var. *sessiliflorum*

Yang LI, Yajiao JIAN, Fan XU, Yongxin LUO, Zhixuan LI, Yi OU, Yan WEN, Jingwei JIN, Chuanrui ZHANG, Lishe GAN

Citation: Yang LI, Yajiao JIAN, Fan XU, Yongxin LUO, Zhixuan LI, Yi OU, Yan WEN, Jingwei JIN, Chuanrui ZHANG, Lishe GAN, Five new terpenoids from *Viburnum odoratissimum* var. *sessiliflorum*, Chinese Journal of Natural Medicines, 2023, 21(4), 298−307. doi: 10.1016/S1875−5364(23)60438−8.

View online: https://doi.org/10.1016/S1875−5364(23)60438−8

Available online at www.sciencedirect.com
ScienceDirect
Chinese Journal of Natural Medicines 2023, **21**(4): 298-307
doi: 10.1016/S1875-5364(23)60438-8
Chinese Journal of Natural Medicines

•Original article•

Five new terpenoids from *Viburnum odoratissimum* var. *sessiliflorum*

LI Yang[1Δ], JIAN Yajiao[2Δ], XU Fan[4], LUO Yongxin[1], LI Zhixuan[1], OU Yi[1], WEN Yan[1], JIN Jingwei[1*], ZHANG Chuanrui[2, 3*], GAN Lishe[1, 4*]

[1] *School of Biotechnology and Health Sciences, International Healthcare Innovation Institute, Wuyi University, Jiangmen 529020, China;*
[2] *Chongqing Key Laboratory of Natural Product Synthesis and Drug Research, School of Pharmaceutical Sciences, Chongqing University, Chongqing 401331, China;*
[3] *Shandong Laboratory of Yantai Drug Discovery, Bohai Rim Advanced Research Institute for Drug Discovery, Yantai 264117, China;*
[4] *College of Pharmaceutical Sciences, Zhejiang University, Hangzhou 310058, China*

Available online 20 Apr., 2023

[ABSTRACT] Five new terpenoids, including two vibsane-type diterpenoids (**1**, **2**) and three iridoid allosides (**3**−**5**), together with eight known ones, were isolated from the leaves and twigs of *Viburnum odoratissimum* var. *sessiliflorum*. Their planar structures and relative configurations were determined by spectroscopic methods, especially 2D NMR techniques. The sugar moieties of the iridoids were confirmed as *β*-D-allose by GC analysis after acid hydrolysis and acetylation. The absolute configurations of neovibsanin Q (**1**) and dehydrovibsanol B (**2**) were determined by quantum chemical calculation of their theoretical electronic circular dichroism (ECD) spectra and $Rh_2(OCOCF_3)_4$-induced ECD analysis. The anti-inflammatory activities of compounds **1**, **3**, **4**, and **5** were evaluated using an LPS-induced RAW264.7 cell model. Compounds **3** suppressed the release of NO in a dose-dependent manner, with an IC_{50} value of 55.64 μmol·L^{-1}. The cytotoxicities of compounds **1**−**5** on HCT-116 cells were assessed and the results showed that compounds **2** and **3** exhibited moderate inhibitory activities with IC_{50} values of 13.8 and 12.3 μmol·L^{-1}, respectively.

[KEY WORDS] *Viburnum odoratissimum* var. *sessilifolrum*; Terpenoids; Acid hydrolysis; ECD calculation; Anti-inflammation
[CLC Number] R284.1 **[Document code]** A **[Article ID]** 2095-6975(2023)04-0298-10

Introduction

The genus *Viburnum* (Adoxaceae) is comprised of about two hundred species worldwide and over seventy of them are distributed in most areas of China [1]. These shrubs or small trees are well-known for their values as ornamentals and medicines. For example, application of the leaves and stems of *V. dilatatum* in traditional Chinese medicine for the treatment of infantile malnutrition can be traced back to the Tang dynasty (618-907).

The plant *V. odoratissimum* and its varietas, including *V. odoratissimum* var. *odoratissimum* and *V. odoratissimum* var. *awabuki*, are widely used in folk medicines to diminish inflammation, relieve pain, and treat rheumatic arthralgia [2-5]. Previous phytochemical investigations on these related species showed the presence of triterpenoids, diterpenoids, sesquiterpenoids, flavonoids, lignans, and coumarin glycosides [6, 7]. Among these constituents, vibsane-type diterpenoids are a rare class of diterpenoids only found in the genus *Viburnum*, which can be further divided into three subtypes: eleven-membered ring, seven-membered ring, and rearranged ring types. Some of these compounds with eleven-membered or seven-membered rings from *V. odoratissimum* exhibited significant cytotoxic activities against tumor cells [8-10]. Furthermore, compounds with the vibsanin B scaffold are found to be a new class of HSP90 C-terminal inhibitors with considerable potential as anticancer agents [11−13]. Total synthesis of all the vibsane-type diterpenoids has been achieved [8, 14, 15].

The evergreen shrub *V. odoratissimum* var. *sessiliflorum*

[Received on] 14-Sep.-2022
[Research funding] This work was supported by the National Natural Science Foundation of China (Nos. 22077111, 22177016, 81872756, and 81901678) and Department of Education of Guangdong Province (No. 2020KZDZX1203).
[*]**Corresponding author]** E-mails: wyuchemjjw@126.com (JIN Jingwei); crzhang@cqu.edu.cn (ZHANG Chuanrui); ganlishe@163.com (GAN Lishe)
[Δ]These authors contributed equally to this work.
These authors have no conflict of interest to declare.

is grown in Yunnan Province of China, Myanmar, and Thailand. In the current study, the chemical constituent of this plant was first investigated and a six-membered ring type vibsane diterpenoid (**1**) and one eleven-membered ring type vibsane diterpenoid (**2**), three new iridoid allosides (**3**–**5**) (Fig. 1), and eight known compounds were isolated from 95% ethanol extracts of *V. odoratissimum* var. *sessiliflorum*. Herein, we report the isolation, structure elucidation, and potential anti-inflammatory activities of these compounds.

Result and Discussion

Compound **1** was isolated as colorless oil. Its molecular formula was determined to be $C_{25}H_{36}O_6$ by a negative HR-ESI-MS pseudo-ion peak at *m/z* 431.2439 $[M - H]^-$ (Calcd. for $C_{25}H_{35}O_6$, 431.2439), with eight indices of hydrogen deficiency (IHDs). The IR spectrum showed absorption bands attributable to unsaturated hydrogens (2925 cm^{-1}), carbonyl (1725 cm^{-1}), and double bond (1668 cm^{-1}) groups. The ^1H NMR data in combination with the HSQC spectrum (Table 1) showed the presence of five methyls at δ_H 2.20 (3H, s, CH_3-4′), 1.94 (3H, s, CH_3-5′), 1.73 (3H, s, CH_3-17), 2.20 (3H, s, CH_3-19), and 0.83 (3H, s, CH_3-20)], three olefinic protons at δ_H 7.15 (1H, d, *J* = 12.3 Hz, H-8), 5.12 (1H, dd, *J* =12.3, 11.1 Hz, H-9), and 5.69 (1H, br s, H-2′), and two oxygen-bearing

Table 1 ^1H (600 MHz) and ^{13}C NMR (150 MHz) data for compounds **1**–**2** (δ in ppm, $CDCl_3$)

No.	1		2	
	δ_H (mult, *J* in Hz)	δ_C	δ_H (mult, *J* in Hz)	δ_C
1	(*α*) 1.53 (m) (*β*) 1.88 (dd, 13.2, 5.7)	41.9	(*α*) 1.90 (m) (*β*) 2.07 (m)	44.9
2	4.32 (m)	64.0	6.02 (dd, 12.5, 3.1)	128.9
3		134.5		143.5
4		136.5		202.6
5	5.08 (m)	83.2	6.08 (d, 16.4)	128.7
6	(a) 2.52 (m) (b) 2.72 (dd, 14.7, 3.5)	47.7	6.56 (d, 16.4)	155.1
7		207.6		74.1
8	7.15 (d, 12.3)	138.1	5.35 (d, 9.0)	81.4
9	5.12 (dd, 12.3, 11.1)	110.9	5.21 (dd, 16.2, 9.0)	124.5
10	2.56 (m)	42.2	5.66 (d, 16.2)	144.7
11		37.9		40.4
12	(a) 1.53 (m) (b) 1.25 (m)	36.1	(a) 2.07 (m) (b) 1.64 (m)	32.4
13	1.53 (m)	29.2	2.67 (m)	32.9
14	4.00 (m)	76.2		202.1
15		147.7		144.5
16	(a) 4.84 (m) (b) 4.95 (m)	111.1	(a) 5.91 (d, 15.1) (b) 5.75 (d, 15.1)	124.8
17	1.73 (3H, s)	17.9	1.87 (3H, s)	17.8
18	(*α*) 4.82 (m) (*β*) 4.61 (d, 12.51)	74.7	(a) 4.41 (d, 12.8) (b) 4.18(d, 12.8)	65.3
19	2.20 (3H, s)	31.3	1.38 (3H, s)	18.4
20	0.83 (3H, s)	21.5	1.02 (3H, s)	23.0
1′		163.3		167.1
2′	5.69 (brs)	114.8	5.78 (brs)	115.7
3′		160.6		159.1
4′	2.20 (3H, s)	20.7	2.19 (3H, s)	20.6
5′	1.94 (3H, s)	27.8	1.93 (3H, s)	27.7

methines at δ_H 4.32 (1H, m, H-2) and 4.00 (1H, m, H-14). The ^{13}C NMR spectrum (Table 1) exhibited twenty-five carbon signals, including a keto carbonyl at δ_C 207.6 (C-7), an ester carbonyl at δ_C 163.3 (C-1′), and eight olefinic carbons for four double bonds (δ_C 134.5, 136.5, 138.1, 110.9, 147.7, 111.1, 114.8, and 160.6). The above data of compound **1** is very similar to those of the known rearranged type vibsane diterpenes with a six-membered ring, neovibsanins H and I, isolated from *V. odoratissimum* [16]. Comparison of their 1D NMR and MS data showed that the *β*,*β*-dimethylacryl enol ester and the acetonyl aliphatic side chain remained unchanged, while the disappearance of 16-methyl and presence of additional olefinic protons around δ_H 4.5–5.0, as well as an additional oxygen-bearing methine proton at δ_H 4.00 (1H, m, H-14) indicated that the dimethyl vinyl side chain $CH_2(12)\cdots CH_3(17)$ in neovibsanin I was metabolized in **1**. Subsequently, analyses of the ^1H–^1H COSY and HSQC spectra of compound **1** allowed the determination of four spin-systems, including $CH_2(1)$-CH(2), CH(5)-$CH_2(6)$, CH(8)-CH(9)-CH(10), and $CH_2(12)$-$CH_2(13)$-CH(14), as depicted in bold bonds in Fig. 2. In the HMBC spectrum (Fig. 2), both the olefinic methylene H_2-16 and the methyl H_3-17 signals showed correlations to the oxygen-bearing methine C-14 at δ_C 76.2, which suggested an isopropenyl terminal connected to the oxygen-bearing C-14 for **1**. In addition, an HMBC correlation from H_2-18 to C-5 confirmed the existence of the dihydrofuran ring. HMBC correlations of H-5/C-7, H-9/C-4, H-9/C-11, and H_2-13/C-11 confirmed the three side chains linked to the bicyclic core. The *β*,*β*-dimethylacryloyloxy group was arranged at C-8 by a key HMBC correlation from H-8 to C-1′. The relative configuration of **1** was determined by ROESY spectrum (Figs. 2 and 3). The *trans* configuration of the C-8/C-9 double bond was determined by a $^3J_{8,9}$ coupling constant value of 12.3 Hz and ROESY correlations (Fig. 3) between H-8 and H-10. ROESY correlations of H_3-20/H-2 and H_3-20/H-9 confirmed their *β*-orientation. ROESY correlations between the *α*-oriented H-10 and H-6a then indicated a *β*-configuration for H-5. The above data verified that the relative configurations on the bicyclic core of **1** were the same as those of neovibsanin I. The absolute configuration of the bicyclic core was confirmed to be 2*R*,5*S*,10*R*,11*S* by quantum chemical calculation of the theoretical ECD spectra. As depicted in Fig. 4, the experimental ECD spectrum and theoretical spectra for both 2*R*,5*S*,10*R*,11*S*,14*S*-**1** and 2*R*,5*S*,10*R*,11*S*,14*R*-**1** showed similar positive Cotton effects (Fig. 4). The absolute configuration of 14-OH on the flexible side chain far from the chromophores of these diterpenoids was not determined in previous literatures [17-19]. Herein, the absolute configuration of the secondary alcohol was assigned by $Rh_2(OCOCF_3)_4$-induced ECD analysis. According to the bulkiness rule for secondary alcohols [20, 21], an enhanced negative Cotton effect around 350 nm in the $Rh_2(OCOCF_3)_4$-induced CD spectrum of **1** implied an *R*-configuration for C-14 (see Supporting Information). The above approaches allowed the determination of the absolute configuration of **1** as 2*R*,5*S*,10*R*,11*S*,14*R*. Thus, the structure of compound **1** was elucidated as shown in Fig. 1 and named neovibsanin Q.

Compound **2** was isolated as colorless oil. The molecular formula was determined to be $C_{25}H_{34}O_6$ on the basis of (−)-HR-ESI-MS data (*m*/*z* 429.2289, $[M - H]^-$, Calcd. for $C_{25}H_{33}O_6$, 429.2283). The IR spectrum suggested the presence of hydroxy group (3442 cm^{-1}) and double bond (1653 cm^{-1}). The ^1H NMR spectrum of **2** (Table 1) showed the presence of two characteristic methyls at δ_H 2.19 (s, CH_3-4′) and

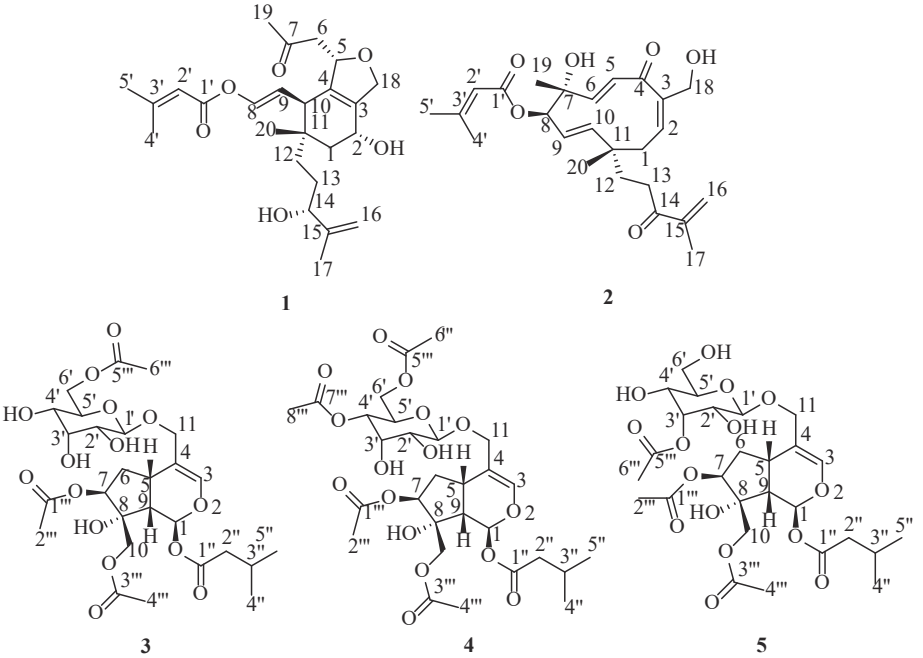

Fig. 1 The structures of compounds 1–5

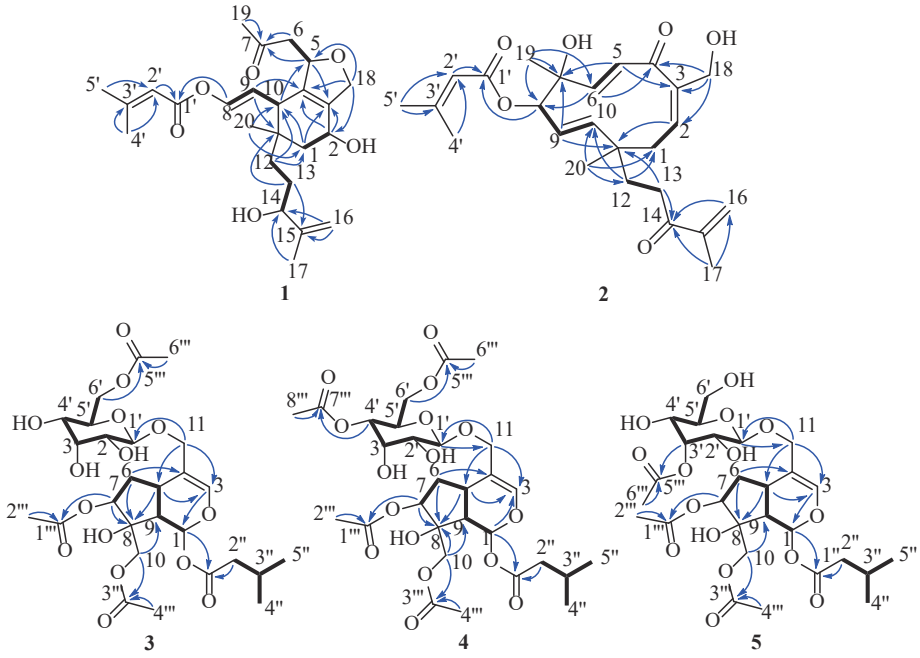

Fig. 2 Key HMBC and ^{1}H–^{1}H-COSY correlations of compounds 1–5

1.93 (s, CH_3-5′), as well as an olefinic proton at δ_H 5.78 (1H, br s, H-2′) for the *β*,*β*-dimethylacryl substituent. Two pairs of olefinic protons at δ_H 6.08 (1H, d, *J* = 16.4 Hz, H-5), 6.56 (1H, d, *J* = 16.4 Hz, H-6), and 5.21 (1H, dd, *J* = 16.2, 9.0 Hz, H-9), 5.66 (1H, d, *J* = 16.2 Hz, H-10) indicated two characteristic trans-configuration di-substituted double bonds for the 11-membered ring type vibsane diterpenoid, similar as that of visbsanol B isolated from *V. odoratissimum* [22]. Furthermore, the presence of an additional keto carbonyl at δ_C 202.1 and the absence of a proton on the oxygen-bearing carbon C-14 around δ_H 4.00, as well as the molecular formula with two less hydrogen atoms, suggested that the hydroxyl was oxygenated to a ketone group at C-14. Subsequently, analyses of the ^{1}H–^{1}H COSY and HSQC spectra of compound **2** allowed the determination of four spin-systems, including CH_2(1)-CH(2), CH(5)-CH(6), CH(8)-CH(9)-CH(10), and CH_2(12)-CH_2(13), as depicted in bold bonds in Fig. 2. In the HMBC spectrum, correlations from H_2-18 to C-2, C-3, and C-4, correlations from H_3-20 to C-11, C-12, C-10, and C-1, and correlations from H_3-19 to C-6, C-7, and C-8 verified an eleven membered ring skeleton. Key HMBC correlations from H_2-16 and H_3-17 to the keto carbonyl at δ_C 202.1 confirmed the ketone group at C-14. The relative configuration of **2** was elucidated by ROESY spectrum (Fig. 3). The ROESY cross-peaks of H_3-19/H-5, H_3-19/H-9, and H-9/H_3-20 revealed that they were co-facial and assigned as *β*. The other key correlations of H-10/H-8 and H-10/H-12a then showed their *α*-orientation. The above ROESY data showed a relative configuration that was the same as that of visbsanol B. The absolute configuration of **2** was also determined by quantum chemical calculation of its theoretical ECD spectrum. In the 200–450 nm region (Fig. 4), both the experimental ECD curve of **2** and the theoretical one for 7*R*,8*R*,11*S*-**2** showed a first positive Cotton effect around 330 nm, a second negative Cotton effect around 260 nm, and a third positive Cotton effect around 230 nm. The high similarity between the experimental and theoretical curves enabled the verification of the absolute configuration of **2** as 7*R*,8*R*,11*S*. Therefore, the structure of compound **2** was determined and named dehydrovibsanol B (Fig. 1).

Compound **3** was isolated as a colorless gum. The molecular formula was found to be $C_{27}H_{40}O_{15}$ on the basis of a negative HR-ESI-MS pseudo-ion peak at *m*/*z* 603.2291 ([M − H]$^-$, Calcd. for $C_{27}H_{39}O_{15}$, 603.2294), indicating eight indices of hydrogen deficiency. The IR spectrum suggested the presence of hydroxyl group (3481 cm^{-1}), ester carbonyl group (1740 cm^{-1}) and double bond (1673 cm^{-1}). The ^{1}H NMR spectrum of **3** (Table 2) exhibited typical resonances for an iridoid acetal proton and an oxygen-bearing olefinic methine proton at δ_H 6.28 (1H, d, *J* = 5.6 Hz, H-1) and 6.41 (1H, s, H-3), respectively. Additionally, an anomeric proton signal for the sugar moiety at δ_H 4.65 (1H, d, *J* = 7.7 Hz, H-1′), three acetoxyl singlets around δ_H 2.10, and two overlapped methyl doublets at δ_H 0.95 (6H, d, *J* = 6.6 Hz, H-4″, H-5″) for an isovaleryl moiety indicated an iridoid structure similar to those of viburnumfocesides A–D, isolated from *Viburnum foetidum* var. *ceanothoides* [23]. The ^{13}C NMR spectrum verified the existence of the characteristic acetal carbon at δ_C 89.1 (C-1) and the oxygen-bearing double bond carbons at δ_C 141.0 (C-3) and 112.3 (C-4). Compared with the 1D NMR spectra of viburnumfoceside A, the absence of the *Z*-*p*-coumaroyl group and the presence of an additional acetyl moiety indicated that the coumaroyl group on the sugar moiety might be replaced by an acetyl group, which also was consistent with the MS data. The ^{1}H–^{1}H COSY and HSQC spectra of compound **3** allowed the determination of three spin-systems

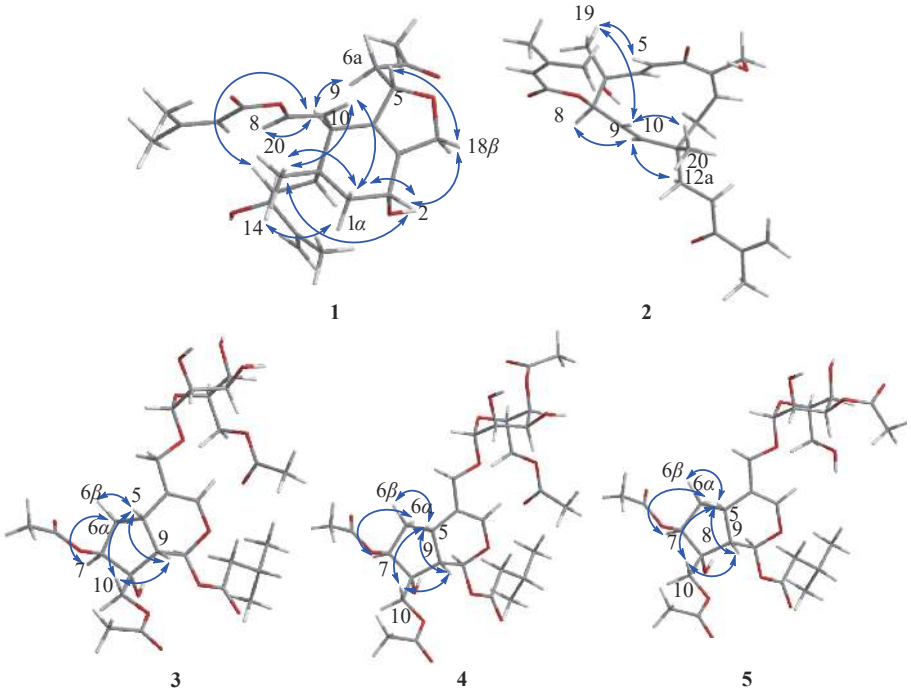

Fig. 3 Selected ROESY correlations of compounds 1–5

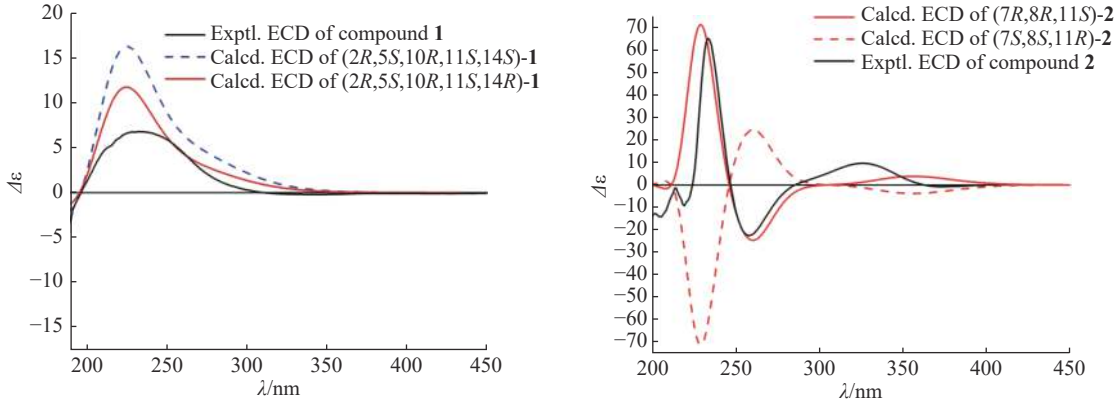

Fig. 4 The experimental and calculated ECD spectra of compounds 1 and 2

depicted as bold bonds in Fig. 2. On the HMBC spectrum, those correlations confirmed the same subunits as those of viburnumfoceside A, while a key signal from the hexose methylene (CH_2-6′) to the acetyl carbonyl carbon at δ_C 171.5 (C-5‴) confirmed the location of the acetoxyl group at C-6′. The relative configuration of **3** was confirmed by the ROESY data (Fig. 3). The *β*-orientation of H-5, H-9, and H_2-10 was confirmed by key ROESY correlations of H-5/H-9, H-5/H-6*β*, and H-9/H_2-10. The ROESY correlations of H-6α/H-7 then verified their *α*-orientation. For the hexose moiety, the anomeric proton resonated at δ_H 4.65 (d, J = 7.7 Hz, H-1′) and the other NMR data suggested the presence of a *β*-D-allopyranosyl group, the same as that of viburnumfoceside A [23]. Furthermore, an acid hydrolysis of **3** and subsequent acetylation and GC analysis showed that the hexose was identical as an authentic sample of D-allose. Therefore, the structure of compound **3** was identified as 11-*O*-(6-*O*-acetyl-*β*-D-allopyranosyl)-7,10-diacetoxy-8-hydroxy-1-isovaleroxy iridoid.

The molecular formula of compound **4** was determined as $C_{29}H_{42}O_{16}$ by HR-ESI-MS data (*m/z* 645.2409, $[M - H]^-$, Calcd. for $C_{29}H_{41}O_{16}$, 645.2400). The IR spectrum showed very similar absorptions as those of **3**. Compared with that of compound **3**, the ^{1}H NMR spectrum of **4** (Table 2) exhibited an additional acetoxyl methyl singlet at δ_H 2.12 (3H, s), which was verified again by the ^{13}C NMR resonances at δ_C 171.3 and 21.0 (Table 3). The above data showed that **4** is an acetylized product of **3**, and the additional acetoxyl group was attached to C-4′ on the allose moiety according to HMBC correlations from H-4′ (δ_H 4.85) to the acetoxyl carbonyl. The relative configuration of **4** was confirmed to be identical with that of **3** by the ROESY correlations depicted as shown in Fig. 3. Therefore, the structure of compound **4** was elucidated as 11-*O*-(4,6-*O*-diacetyl-*β*-D-allopyranosyl)-7,10-di-

Table 2 ^{1}H NMR data for compounds 3–5 (600 MHz, δ in ppm, *J* in Hz, $CDCl_3$)

No.	3	4	5
1	6.28 (d, 5.6)	6.30 (d, 5.6)	6.29 (d, 5.6)
3	6.41 (s)	6.42 (br s)	6.43 (br s)
5	2.89 (m)	2.92 (m)	2.91 (m)
6	(*α*) 1.91 (m)	(*α*) 1.92 (m)	(*α*) 1.94 (m)
	(*β*) 2.42 (m)	(*β*) 2.40 (m)	(*β*) 2.36 (m)
7	5.08 (t, 5.9)	5.08 (t, 6.1)	5.04 (t, 5.8)
9	2.42 (m)	2.44 (m)	2.42 (m)
10	4.21 (br s)	4.21 (br s)	4.21 (br s)
11	(a) 4.25 (d, 11.8)	(a) 4.30 (d, 11.8)	(a) 4.28 (d, 11.8)
	(b) 4.06 (d, 12.0)	(b) 4.06 (d, 11.8)	(b) 4.08 (d, 11.6)
1′	4.65 (d, 7.7)	4.72 (d, 7.8)	4.68 (d, 7.8)
2′	3.44 (dd, 8.0, 2.9)	3.53 (dd, 7.9, 3.1)	3.60 (dd, 7.6, 2.7)
3′	4.20 (m)	4.36 (t, 2.5)	5.55 (t, 3.0)
4′	3.52 (brd)	4.85 (dd, 10.1, 2.5)	3.85 (dd, 9.2, 2.7)
5′	3.80 (m)	4.12 (m)	3.70 (m)
6′	(a) 4.38 (dd, 12.3, 2.1)	(a) 4.26 (dd, 12.2, 4.9)	(a) 3.78 (dd, 11.9, 4.5)
	(b) 4.29 (dd, 11.7, 4.2)	(b) 4.18 (dd, 12.1, 1.7)	(b) 3.87 (m)
2″	2.21 (d, 7.2)	2.22 (d, 7.2)	2.23 (d, 7.2)
3″	2.06 (m)	2.10 (m)	2.10 (m)
4″	0.95 (3H, s)	0.97 (3H, s)	0.95 (3H, s)
5″	0.95 (3H, s)	0.97 (3H, s)	0.95 (3H, s)
2‴	2.09 (3H, s)	2.07 (3H, s)	2.11 (3H, s)
4‴	2.06 (3H, s)	2.12 (3H, s)	2.05 (3H, s)
6‴	2.10 (3H, s)	2.07 (3H, s)	2.19 (3H, s)
8‴	-	2.12 (3H, s)	-

acetoxy-8-hydroxy-1-isovaleroxy iridoid.

Compound **5** exhibited the same molecular formula and similar IR spectrum as those of **3**. Comparison of the ^{1}H NMR spectra of **5** and **3** (Table 2) showed that the signals of the acetylized 6′-CH_2O in **3** were shifted to higher field at δ_H 3.87 (dd, *J* = 11.9, 4.5 Hz) and 3.78 (dd, *J* = 11.8, 2.7 Hz), and the 3′-CH-O signal was strongly shifted to lower field at δ_H 5.55 (m), which indicated that the acetoxyl group at C-6′ in **3** was shifted to C-3′ in compound **5**. HMBC correlations from H-3′ to the acetoxyl carbonyl C-5‴ and the anomeric carbon C-1′ confirmed the position of the acetoxyl group on the allose moiety. The structure of compound **5** was finally determined to be 11-*O*-(3-*O*-acetyl-*β*-D-allopyranosyl)-7,10-diacetoxy-8-hydroxy-1-isovaleroxy iridoid.

Through spectroscopic analysis and comparison with the reported data in the literature, the structures of the known compounds were determined as three eleven-membered ring type vibsane diterpenoids, vibsanol A (**6**) [22], vibsanol B (**7**) [22], and 15-*O*-methylvibsanol A (**8**) [24], three seven-membered ring type vibsane diterpenoids, vibsanin H (**9**) [25], dehydrovibsanin G (**10**) [25], and vibsanin G (**11**) [17], and two iridoids, opulus iridoid I (**12**) [26] and 7,10,2′,3′-tetraacetylus-pensolide F (**13**) [27].

The anti-inflammatory activity of compounds **1**, **3**, **4**, and **5** was evaluated using a lipopolysaccharide (LPS)-stimulated RAW264.7 macrophage cell model. The cytotoxicity of compounds **1**, **3**, **4**, and **5** on RAW264.7 cells were first evaluated by MTT assay. Compounds **1**, **4**, and **5** had no obvious cytotoxicity, while compound **3** exhibited slight cytotoxicity in the range of 40–160 μmol·L^{-1}. For the inhibitory effect on NO production, compounds **3** and **5** dose-dependently inhibited the NO level in the range of 10−160 μmol·L^{-1} and compound **3** exhibited an IC_{50} of 55.64 ± 3.39 μmol·L^{-1}, which indicated that the two compounds had weak anti-inflammatory effect (see Supporting Information). The above data also indicated that substituents can obviously affect the activity and cytotoxicity of these iridoids and the NO inhibitory effect of compound **3** may partially be induced by its cytotox-

Table 3 ^{13}C NMR data for compounds 3–5 (150 MHz, δ in ppm, $CDCl_3$)

No.	3	4	5
1	89.1	89.2	89.3
3	141.0	141.0	140.8
4	112.3	112.7	112.7
5	31.7	31.5	31.3
6	34.0	34.1	34.0
7	81.2	81.4	81.1
8	80.3	80.4	80.3
9	44.7	44.9	44.6
10	67.4	67.6	67.3
11	68.8	69.3	69.0
1′	98.7	99.5	99.5
2′	70.9	70.7	69.7
3′	70.6	69.0	73.1
4′	67.5	68.8	67.7
5′	72.0	69.6	74.0
6′	64.0	62.9	62.4
1″	171.3	171.1	171.3
2″	43.2	43.4	43.4
3″	25.6	25.8	25.8
4″	22.3	22.5	22.3
5″	22.3	22.5	22.3
1‴	171.1	170.9	170.9
2‴	20.9	21.1	21.0
3‴	171.0	171.1	171.0
4‴	21.0	21.0	20.7
5‴	171.5	171.2	172.0
6‴	20.7	21.2	21.0
7‴	-	171.3	-
8‴	-	21.0	-

icity on RAW264.7 macrophage cells.

A cytotoxic activity assay on HCT-116 human colorectal adenocarcinoma cells was also performed for compounds **1**–**5**. The results showed that compounds **2** (IC_{50} 13.8 μmol·L^{-1}) and **3** (IC_{50} 12.3 μmol·L^{-1}) exhibited moderate inhibitory activity against the proliferation of HCT-116 cells.

Experimental

General experimental procedures

Optical rotation values were obtained on a Jasco P-1010 polarimeter. UV spectra were measured on a Shimadzu UV-1601 UV-Vis spectrometer. IR spectra were measured on a Shimadzu FTIR-8300 spectrometer using KBr disks. ESIMS data were measured on a Bruker Apex-ultra FT-ICR spectrometer. ECD spectra were measured on a MOS-450 CD spectrometer. NMR spectra were measured on an Agilent 600 MR DD2 spectrometer (Agilent Co., USA) with TMS as the internal standard. Column chromatography (CC) were performed using silica gel (100–200 mesh, 200–300 mesh and 300–400 mesh, Yantai Jiangyou Silicone Development Co., Ltd., Yantai, China), MCI gel (CHP20P, 75–150 μm, Mitsubishi Chemical Industries Ltd., Japan), and Sephadex LH-20 gel (25–100 μm, GE Healthcare Bio-Sciences AB, Sweden). All solvents used for CC were of analytical grade (Tianjin Fuyu Fine Chemical Co., Ltd., Tianjin, China) and those used for HPLC were of HPLC grade (Oceanpak Alexative Chemical Ltd., Goteborg, Sweden). Pre-coated silica gel GF_{254} plates (Qingdao Haiyang Chemical Co., Ltd., Qingdao, China) were used for thin-layer chromatography (TLC). The clean bench and CO_2 incubator were from Esco Micro Pte. Ltd. (Singapore).

Plant material

The leaves and twigs of *Viburnum odoratissimum* var. *sessilifolrum* were collected in Xishuangbanna Tropical Botanical Garden in May 2018 and authenticated by Prof. XU Youkai from Xishuangbanna Tropical Botanical Garden, Chinese Academy of Sciences. A specimen (CRZ2018 VOVS) was stored in School of Pharmaceutical Sciences, Chongqing University.

Extraction and isolation

The air-dried twigs and leaves of *Viburnum odoratissimum* var. *sessilifolrum* (6.2 kg) were powdered and extracted with 95% ethanol at room temperature for three times, each time for 3 d. The solvent was removed under reduced pressure to obtain a crude extract (524.0 g), which was then dissolved in distilled water and extracted with petroleum ether, ethyl acetate, and *n*-butanol successively. The ethyl acetate fraction (95.7 g) was subjected to an MCI gel column eluted with MeOH–H_2O (40 ∶ 1 to 100 ∶ 1, *V*/*V*) to give five subfractions Frs. 1–5. Fr. 2 (9.7 g) was further separated on a silica gel column (CH_2Cl_2–MeOH, 1 ∶ 1, *V*/*V*) and later a semi-preparative column (250 mm × 10 mm, 5 μm) by HPLC (CH_3CN–H_2O, 4 ∶ 6 to 10 ∶ 0, *V*/*V*, 2 mL·min^{-1}) to obtain compound **3** (t_R = 13.9 min, 100.5 mg), compound **4** (t_R = 16.6 min, 1.5 mg), compound **5** (t_R = 15.3 min, 8.6 mg), compound **12** (t_R = 11.6 min, 10.9 mg), and compound **13** (t_R = 14.5 min, 10.3 mg). Fr. 3 (6.5 g) was subjected to a silica gel column (CH_2Cl_2–MeOH, 1 ∶ 1, *V*/*V*) and later a semi-preparative column (250 mm × 10 mm, 5 μm) on HPLC (CH_3CN–H_2O, 5 ∶ 5 to 10 ∶ 0 *V*/*V*, 2 mL·min^{-1}) to obtain compound **2** (t_R = 18.3 min, 7.8 mg), compound **6** (t_R = 19.6 min, 8.6 mg), compound **7** (t_R = 16.5 min, 8.5 mg) and compound **8** (t_R = 16.6 min, 8.6 mg). Fr. 4 (3.8 g) was also subjected to a silica gel column (CH_2Cl_2–MeOH, 1 ∶ 1, *V*/*V*) and later a semi-preparative column (250 mm × 10 mm, 5 μm) by HPLC (MeOH –H_2O, 6 ∶ 4 to 10 ∶ 0, *V*/*V*, 2

mL·min^{-1}) to obtain compound **1** (t_R = 22.4 min, 3.1 mg), compound **9** (t_R = 24.6 min, 8.9 mg), compound **10** (t_R = 25.7 min, 6.1 mg), and compound **11** (t_R = 23.5 min, 5.9 mg).

Identification of new compounds

*Neovibsanin Q (**1**)*

Colorless oil; $[\alpha]_D^{25}$ +188.2 (*c* 0.085, MeOH); CD (*c* 0.05 mg·mL^{-1}, MeOH) λ_{max} ($\Delta\varepsilon$) 223 (+5.89);(−)-HR-ESI-MS *m/z* 431.2439 [M − H]$^-$ (Calcd. for $C_{25}H_{35}O_6$, 431.2439); IR (KBr) ν_{max}: 2925, 2855, 1725, 1668, 1460, 1222, 1140, 1092, 948 cm^{-1}; ^{1}H and ^{13}C NMR data: see Table 1.

*Dehydrovibsanol B (**2**)*

Colorless oil; $[\alpha]_D^{27}$ −147.0 (*c* 0.1, MeOH); CD (*c* 0.1 mg·mL^{-1}, MeOH) λ_{max} ($\Delta\varepsilon$) 234 (+65.38), 259 (−22.51), 327 (+9.62); (−)-HR-ESI-MS *m/z* 429.2289 [M − H]$^-$ (Calcd. for $C_{25}H_{33}O_6$, 429.2283); UV (MeOH) λ_{max} (log ε): 258(3.19) nm; IR (KBr) ν_{max}: 3442, 2927, 1653, 1451, 1379, 1227, 1146, 1082, 999, 853, 736 cm^{-1}; ^{1}H and ^{13}C NMR data: see Table 1.

*11-*O*-(6-*O*-acetyl-β-D-allopyranosyl)-7,10-diacetoxy-8-hydroxy-1-isovaleroxy iridoid (**3**)*

Colorless gum; $[\alpha]_D^{24.2}$ −33.5 (*c* 0.275, MeOH); (−)-HR-ESI-MS *m/z* 603.2291 [M − H]$^-$ (Calcd. for $C_{27}H_{39}O_{15}$, 603.2294); IR (KBr) ν_{max}: 3481, 2960, 2929, 1740, 1673, 1440, 1375, 1248, 1148, 1095, 1038, 936, 736, 606 cm^{-1}; ^{1}H and ^{13}C NMR data: see Tables 2 and 3.

*11-*O*-(4,6-*O*-diacetyl-β-D-allopyranosyl)-7,10-diacetoxy-8-hydroxy-1-isovaleroxy iridoid (**4**)*

Colorless gum; $[\alpha]_D^{23.8}$ −28 (c 0.025, MeOH); (−)-HR-ESI-MS *m/z* 645.2409 [M − H]$^-$ (Calcd. for $C_{29}H_{41}O_{16}$, 645.2400); IR (KBr) ν_{max}: 3359, 3194, 2925, 2854, 1742, 1665, 1463, 1374, 1252, 1146, 1096, 1036, 863, 805, 738 cm^{-1}; ^{1}H and ^{13}C NMR data: see Tables 2 and 3.

*11-*O*-(3-*O*-acetyl-β-D-allopyranosyl)-7,10-diacetoxy-8-hydroxy-1-isovaleroxy iridoid (**5**)*

Colorless gum; $[\alpha]_D^{22.7}$ −32 (c 0.1, MeOH); (−)-HR-ESI-MS *m/z* 603.2298 [M − H]$^-$ (Calcd. for 603.2294, $C_{27}H_{39}O_{15}$); IR (KBr) ν_{max}: 3500, 3331, 2927, 2858, 1740, 1674, 1607, 1460, 1375, 1251, 1147, 1093, 1039, 935, 736, 605 cm^{-1}; ^{1}H and ^{13}C NMR data: see Tables 2 and 3.

*Acid hydrolysis, acetylation, and GC analysis of compounds **3**−**5***

Each compound (1−2 mg) was hydrolyzed with 2 mol·L^{-1} HCl (4 mL) at 90 °C for 2 h. The reaction mixture was extracted with ethyl acetate for three times. The ethyl acetate layer was removed and the aqueous layer was evaporated to dryness and then dissolved in anhydrous pyridine (0.4 mL). Hydroxylamine hydrochloride (5 mg) was added into the mixture and kept at 90 °C for 1 h. Acetic anhydride (0.6 mL) was then added and stirred at 90 °C for another 1 h. The reaction mixture was directly analyzed by GC-MS. The sugar moieties of compounds **3**−**5** were determined by comparing the retention times with the derivatives of standard sugars prepared by the same protocol.

GC-MS conditions: the temperature of the injector, 270 °C; injection volume, 1.0 μL; split ratio, 10 ∶ 1; carrier gas, helium at a flow rate of 1.0 mL·min^{-1}; chromatographic column, hp-5ms (250) μm × 30 m, 0.25 μm; column temperature, 160 °C (2 °C·min^{-1}), 195 °C (10 °C·min^{-1}, 6 min), and 300 °C (5 min); and detector: FID 280 °C (nitrogen volume 30 mL·min^{-1}, hydrogen volume flow 40 °C·min^{-1}, and air volume flow 3400 mL·min^{-1}).

The retention times for standard sugar derivatives were t_R = 13.517 min (D-allose), t_R = 14.623 min (D-glucose), t_R = 14.197 min (D-mannose), t_R = 15.282 min (D-fructose), and t_R = 14.524 min (D-sorbose). The retention times for the reaction products of compounds **3**, **4**, and **5** were t_R = 13.378 min (**3**), t_R = 13.336 min (**4**), and t_R = 13.372 min (**5**), respectively. A mixture sample of reaction products from D-allose and compound **3** showed one peak at t_R = 13.465 min (see Fig. 42−50 in supplementary materials).

*Quantum chemical calculation of ECD spectra of **1** and **2***

Conformational analysis was first performed through Monte Carlo searching using molecular mechanics with MMFF force field in the Spartan 18 program [28]. The results showed seven lowest energy conformers for 2*R*,5*S*,10*R*,11*S*,14*S*-**1** and six ones for 2*R*,5*S*,10*R*,11*S*,14*R*-**1** within an energy window of 2.0 Kcal·mol^{-1}, and eleven lowest energy conformers for 7*R*,8*R*,11*S*-**2** within an energy window of 1.5 Kcal·mol^{-1}. Those conformers were then reoptimized using DFT at the B3LYP/6-31G(d) level using the Gaussian 09 program [29]. The B3LYP/6-31G(d) harmonic vibrational frequencies were further calculated to confirm their stability and six conformers for 2*R*,5*S*,10*R*,11*S*,14*S*-**1**, two conformers for 2*R*,5*S*,10*R*,11*S*,14*R*-**1**, and seven conformers for 7*R*,8*R*,11*S*-**2** (See supporting information) were refined and considered for next steps.

The electronic excitation energies and rotatory strengths (velocity) of the first 60 excited states of these conformers were calculated using the TDDFT methodology at the M062X/TZVP level in gas phase. The ECD spectra were simulated by the overlapping Gaussian function [30] (σ = 0.55 eV and + 15 nm shifted in the horizontal axis for **1**; σ = 0.3 eV and −15 nm shifted in the horizontal axis for **2**), in which the velocity rotatory strengths of the first four exited states for **1** and eight exited states for **2** were adopted. To get the final ECD spectra, the simulated spectra of the lowest energy conformers were averaged according to the Boltzmann distribution theory and their relative Gibbs free energy (ΔG). The theoretical ECD curve of 7*S*, 8*S*, 11*R*-**2** was obtained by directly reversing that of 7*R*, 8*R*, 11*S*-**2**.

*Determination of the absolute configuration at C-14 of **1** by $Rh_2(OCOCF_3)_4$-induced ECD*

Compound **1** (0.25 mg) was dissolved in anhydrous CH_2Cl_2 (0.5 mL) and mixed with [$Rh_2(OCOCF_3)_4$] [molar ratio *ca.* 1 ∶ 2 secondary alcohol/[$Rh_2(OCOCF_3)_4$]. Then, the first ECD spectrum was immediately measured from 190 nm to 450 nm, and its time evolution was monitored until stable phase (about 30 min). The induced ECD (IECD) spectrum was subtracted from the inherent ECD spectrum. The observed sign of the band around 350 nm in the induced CD

spectrum was correlated to the absolute configuration of the secondary alcohol [20, 21].

Anti-inflammatory activity assay

The anti-inflammatory assay was performed according to the protocol reported in a lipopolysaccharide (LPS)-stimulated RAW264.7 macrophage cell model and the content of inflammatory mediator NO was measured to evaluate the levels of inflammatory response [31, 32]. Briefly, mouse derived RAW264.7 macrophages were cultured and MTT assay was performed to evaluate the effect of all the compounds on cell viability. The cells were seeded in 96-well plates with an initial density of 5×10^3 cells/mL, before treatment with different concentrations of compounds **1** and **3**–**5** (10, 20, 40, 80, and 160 μmol·L^{-1}) for 1 h. Subsequently, 10 μL of MTT (5 mg·mL^{-1}) solution was added to each well and the microplate was incubated for 4 h. For LPS-stimulation, after treatment with compounds for 2 h, 2 μg·mL^{-1} LPS was added and the cells were cultured for 24 h to evaluate inhibitory effect. Dexamethasone (DXM, 0.2 and 0.4 μmol·L^{-1}) was used as the positive control. The content of NO was measured using Griess reagent. All the experiments were performed in triplicate. Data are expressed as mean ± standard deviation (SD). Values were considered statistically significant when $P < 0.05$.

Cytotoxic activity assay on HCT-116 cells

The viability of HCT-116 human colorectal adenocarcinoma cells was measured by MTT assay [33]. The cells were seeded in 96-well plates (Nalge Nunc International, Rochester, NY, USA) at a density of 1×10^4 cells/well. After incubation for 24 h, the cells were treated with various concentrations (1, 10, 25, 50, and 100 μmol·L^{-1}) of compounds **1**–**5** for 24 h. Then, MTT solution (100 μL) was added to each well and the cells were incubated in a humidified incubator at 37 °C for 4 h. The formed formazan crystals were dissolved with DMSO. The absorbances of each sample was measured at a wavelength of 540 nm using a microplate reader (Model 680; Bio-Rad Laboratories, Inc., Hercules, CA, USA). Doxorubicin (IC_{50} 0.36 μmol·L^{-1}) was used as the positive control.

Supporting Information

Supporting information of this paper can be requested by sending E-mail to the corresponding author.

References

[1] Wang LQ, Chen YG, Xu JJ, *et al*. Compounds from *Viburnum* species and their biological activities [J]. *Chem Biodivers*, 2008, **5**: 1879-1899.

[2] Shen YQ, Lin CL, Chien SC, *et al*. Vibsane diterpenoids from the leaves and flowers of *Viburnum odoratissimum* [J]. *J Nat Prod*, 2004, **67**(1): 74-77.

[3] Liu J, Zhou WB, Cong YW, *et al*. Research progress on chemical constituents and biological activities of coral trees [J]. *Acta Pharm Sin*, 2013, **48**(3): 325-332.

[4] Ma JZ, Yang XW, Zhang JJ, *et al*. Sterols and terpenoids from *Viburnum odoratissimum* [J]. *Nat Product Bioprosp*, 2014, **4**: 175-180.

[5] Zhang Y, Zhou WY, Song XY, *et al*. Neuroprotective terpenoids from the leaves of *Viburnum odoratissimum* [J]. *Nat Prod Res*, 2018, **34**: 1352-1359.

[6] Kawazu KB. Isolation of vibsanines A, B, C, D, E and F from *Viburnum odoratissimum* [J]. *Agric Biol Chem*, 1980, **44**(6): 1367-1372.

[7] Wang XY, Shi HM, Li XB, *et al*. Chemical constituents of plants from the genus *Viburnum* [J]. *Chem Biodivers*, 2010, **7**: 567-593.

[8] Takao KI, Tsunoda K, Kurisu T, *et al*. Total synthesis of (+)-vibsanin A [J]. *Org Lett*, 2015, **17**: 756-759.

[9] Li SF, Yu XQ, Li YL, *et al*. Vibsane-type diterpenoids from *Viburnum odoratissimum* and their cytotoxic activities [J]. *Bioorg Chem*, 2020, 104498.

[10] Fukuyama Y, Kubo M, Esumi T, *et al*. Chemistry and biological activities of vibsane-type diterpenoids [J]. *Heterocycles*, 2010, **81**(7): 1571.

[11] Ye BX, Deng X, Shao LD, *et al*. Vibsanin B preferentially targets HSP90*β*, inhibits interstitial leukocyte migration, and ameliorates experimental autoimmune encephalomyelitis [J]. *J Immunol*, 2015, **194**: 4489-4497.

[12] He J, Peng LY, Tu L, *et al*. Vibsane-type diterpenes from leaves and twigs of *Viburnum odoratissimum* [J]. *Fitoterapia*, 2016, **109**: 224-229.

[13] Shao LD, Su J, Ye BX, *et al*. Design, synthesis, and biological activities of vibsanin B derivatives: a new class of HSP90 C-terminal inhibitors [J]. *J Med Chem*, 2017, **60**: 9053-9066.

[14] Kubo M, Esumi T, Imagawa H, *et al*. *Chemical Diversity of Vibsane-type Diterpenoids and Neurotrophic Activity and Synthesis of Neovibsanin* [M]. *In Rahman A:* Studies in Natural Products Chemistry, Elsevier, 2014: 41-78.

[15] Matsuki W, Miyazaki S, Yoshida K, *et al*. Synthesis and evaluation of biological activities of vibsanin A analogs [J]. *Bioorg Med Chem Lett*, 2017, **27**: 4536-4539.

[16] Fukuyama Y, Minami H, Yamamoto I, *et al*. Neovibsanins H and I, novel diterpenes from *Viburnum awabucki* [J]. *Chem Pharm Bull*, 1998, **46**(3): 545-547.

[17] Minami H, Anzaki S, Kubo M, *et al*. Structures of new seven-membered ring vibsane-type diterpenes isolated from leaves of *Viburnum awabuki* [J]. *Chem Pharm Bull*, 1998, **46**(8): 1194-1198.

[18] Kubo M, Chen IS, Fukuyama Y. Vibsane-type diterpenes from Taiwanese *Viburnum odoratissimum* [J]. *Chem Pharm Bull*, 2001, **49**(2): 242-245.

[19] El-Gamal AAH, Wang SK, Duh CY. New diterpenoids from *Viburnum awabuki* [J]. *J Nat Prod*, 2004, **67**: 333-336.

[20] Michael G, Gunter S. Circular dichroism, XCIII determination of the absolute configuration of alcohols, olefins, epoxides, and ethers from the CD of their " *in situ*" complexes with [$Rh_2(OCOCF_3)_4$] [J]. *Tetrahedron: Asymmetry*, 1990, **1**(4): 221-236.

[21] Shaker S, Sang J, Yan XL, *et al*. Diterpenoids from *Euphorbia royleana* reverse P-glycoprotein-mediated multidrug resistance in cancer cells [J]. *Phytochemistry*, 2020, **176**: 112395.

[22] Shen YC, Prakash CVS, Wang LT, *et al*. New vibsane diterpenes and lupane triterpenes from *Viburnum odoratissimum* [J]. *J Nat Prod*, 2002, **65**(7): 1052-1055.

[23] Wang DM, Yang Y, Shi XK, *et al*. Viburnumfocesides A–D, 1-*O*-isovaleroylated iridoid 11-*O*-alloside derivatives from *Viburnum foetidum* var. *ceanothoides* [J]. *Fitoterapia*, 2020, **143**: 104601.

[24] Chen XQ, Li Y, He J, *et al*. Triterpenoids and diterpenoids from *Viburnum chingii* [J]. *Chem Pharm Bull*, 2011, **59**(4): 496-498.

[25] Li FJ, Yu HL, Wang GC, *et al*. Diterpenes and lignans from *Vi-*

burnum odoratissimum var. *odoratissimum* [J]. *J Asian Nat Prod Res*, 2015, **42**(3): 1-7.
[26] Bock K, Jensen SR, Juhl B, *et al*. Iridoid allosides from *Viburnum opulus* [J]. *Phytochemistry*, 1978, **17**: 753-757.
[27] Tomassini L, Foddai S, Nicoletti M, *et al*. Iridoid glucosides from *Viburnum ayavacense* [J]. *Phytochemistry*, 1997, **46**(5): 901-905.
[28] *Spartan'18 Tutorial and User's Guide*. Irvine, CA, USA: Wavefunction, Inc., 2019
[29] Frisch MJ, Trucks GW, Schlegel HB, *et al*. *Gaussian 09*, Revision A. 1, Gaussian Inc., Wallingford CT, 2009.
[30] Stephens PJ, Harada N. ECD cotton effect approximated by the Gaussian curve and other methods [J]. *Chirality*, 2010, **22**: 229-233.
[31] Jin JW, He H, Zhang XY, *et al*. The *in vitro* and *in vivo* study of oleanolic acid indole derivatives as novel anti-inflammatory agents: synthesis, biological evaluation, and mechanistic analysis [J]. *Bioorg Chem*, 2021, **113**: 104981.
[32] Ke JH, Zhang LS, Chen SX, *et al*. Benzofurans from *Eupatorium chinense* enhance insulin-stimulated glucose uptake in C2C12 myotubes and suppress inflammatory response in RAW264.7 macrophages [J]. *Fitoterapia*, 2019, **134**: 346-354.
[33] Ren J, Cheng H, Wen QX, *et al*. Induction of apoptosis by 7-piperazinethylchrysin in HCT-116 human colon cancer cells [J]. *Oncol Rep*, 2012, **28**: 1719-1726.

Cite this article as: LI Yang, JIAN Yajiao, XU Fan, LUO Yongxin, LI Zhixuan, OU Yi, WEN Yan, JIN Jingwei, ZHANG Chuanrui, GAN Lishe. Five new terpenoids from *Viburnum odoratissimum* var. *sessiliflorum* [J]. *Chin J Nat Med*, 2023, **21**(4): 298-307.